Project title: High Performance High Current CW polarized photocathodes for Electron Ion Colliders

Structured Materials Industries, Inc
201 Circle Drive North – Unit # 102
Piscataway, NJ 08854
p: (732) 302-9274, web: www.smicvd.com

Corporate Official:
Dr. Gary S. Tompa, President
p: (732) 302-9274, e: GSTompa@aol.com

Principle Investigator (PI):
Dr. Kannan Vasudevan, Scientist
p: (732) 302-9274, e: kannan.vasudevan@gmail.com

Subcontractors:
Dr. Luca Cultrera, BNL
Mr. Zane Shellenbarger, SRI

Contract No: DE-SC0022416
Presentation Date: 07/29/2025
SMI Contract No.: 42199

FY25 NP SBIR/STTR PI Exchange Mtg
Phase II Technical Point of Contact:
Michelle Shinn, e: Michelle.Shinn@science.doe.gov

Need Addressed: *Higher Performance Photocathodes for Spin Polarized Sources*

- ***Electron Ion Colliders (EIC)*** *need high efficiency, narrow energy distribution source of spin-polarized electrons for examining properties of fundamental particles such as Quarks, Nuclei, Bosons, etc.*
- *Enhanced photoemission properties will also benefit the current and future operation of* ***CEBAF at Jefferson National Laboratory (JLab)*** *as well as future projects at other facilities such as Cornell University,*

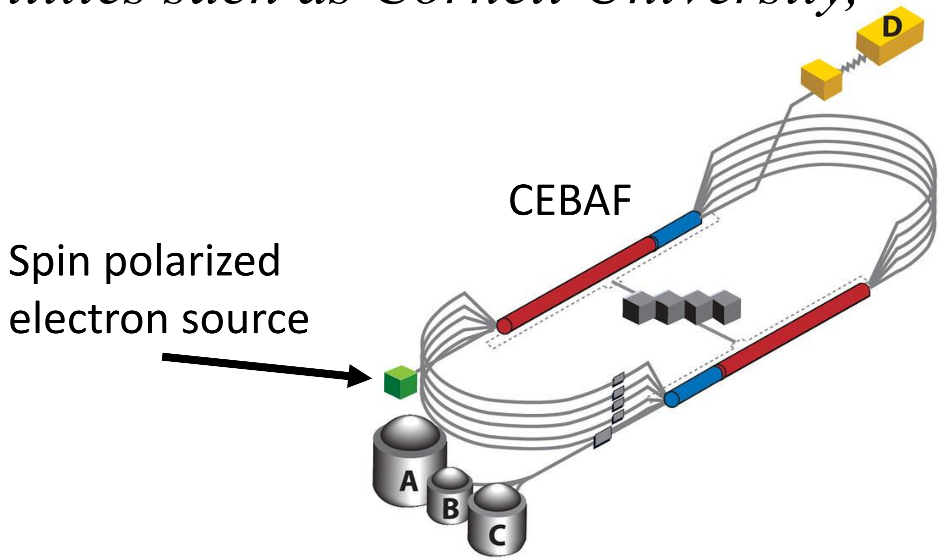

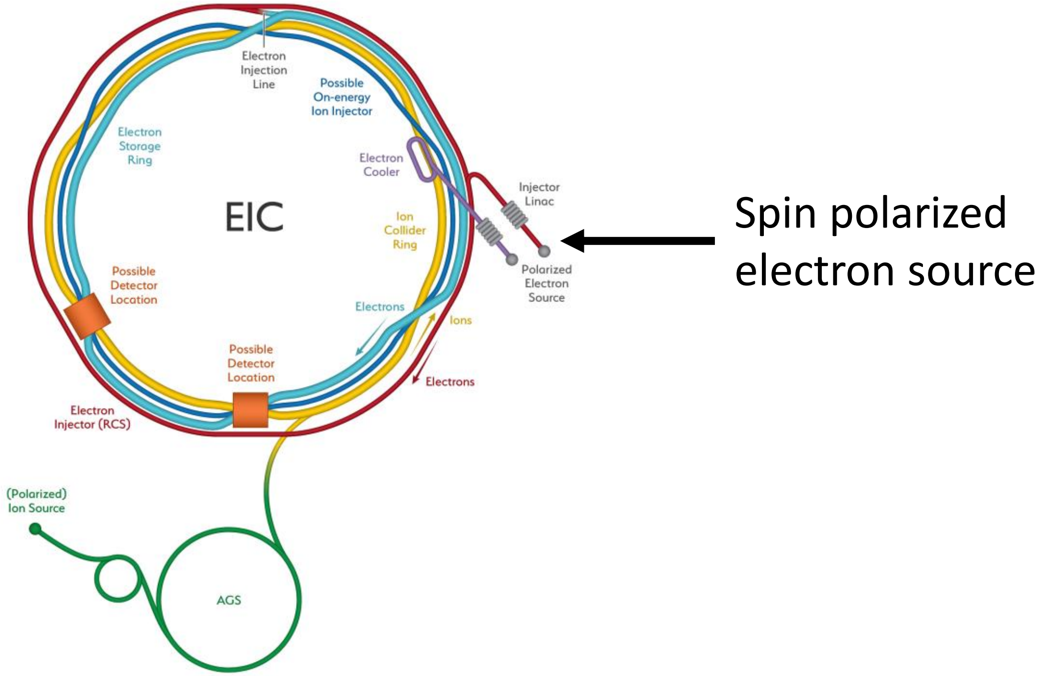

BNL Photocathode system allows characterization for QE and ESP

The load lock system allow us to exchange samples without breaking the vacuum of the activation and polarimeter vacuum chambers.

The UHV system (10^{-11} Torr) consist of three vacuum chambers:
the load lock
the activation chamber
the Mott polarimeter chamber

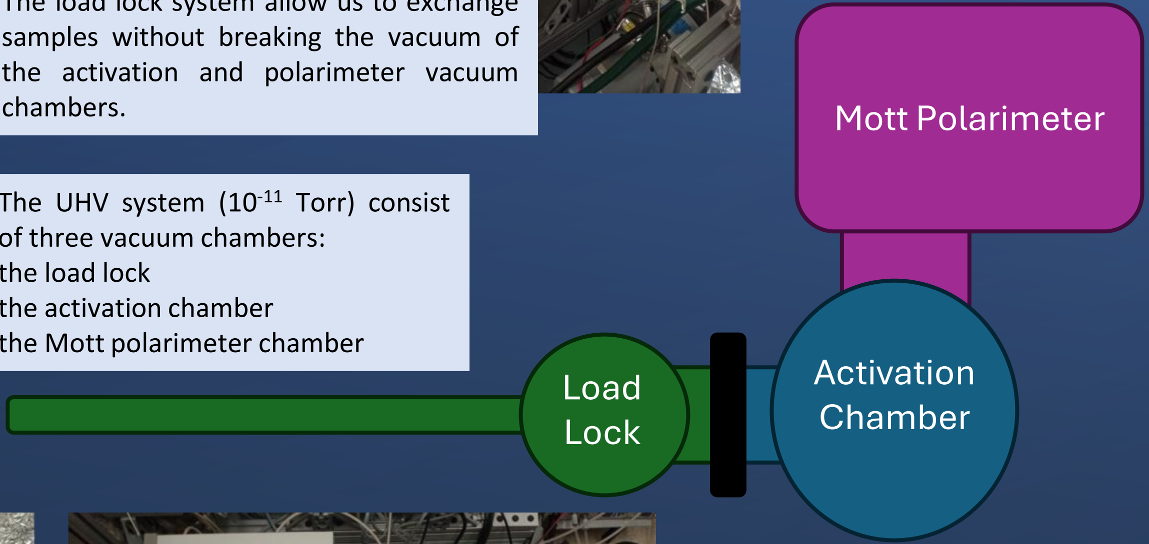

The retarding field Mott polarimeter is operated with an Au target maintained at a voltage of 25 kV.
It allows operation with up to 4 channeltrons detectors for the measure of the electron spin polarization.
For III-V semiconductors measurement only two channeltrons are used.

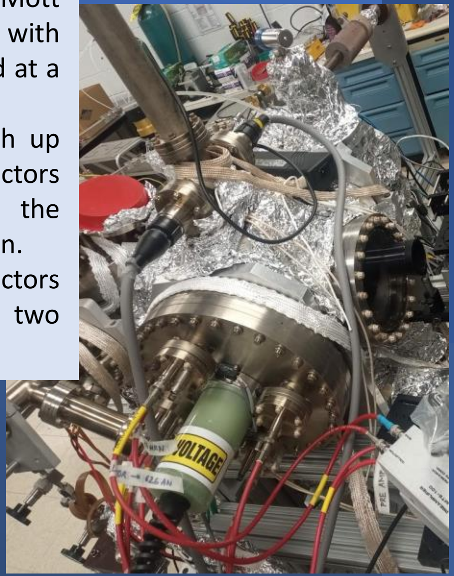

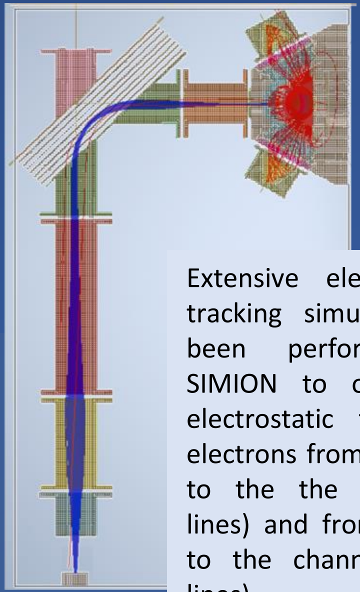

Extensive electron beam tracking simulations have been performed using SIMION to optimize the electrostatic transport of electrons from the cathode to the the target (blue lines) and from the target to the channeltrons (red lines).

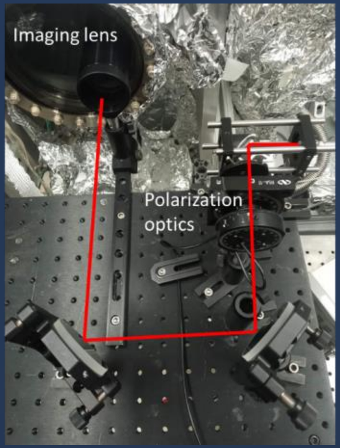

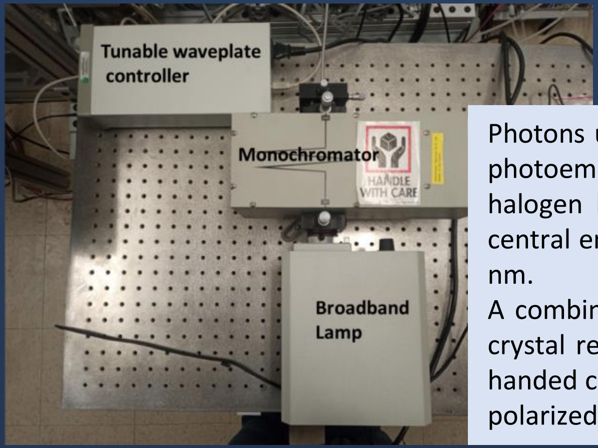

Photons used to illuminate the photocathode during the photoemission experiments are produced by a tungsten halogen lamp. A monochromator is used to select the central emission wavelength with bandwidth of about 10 nm.
A combination of a linear polarizer and a tunable liquid crystal retarder are used to produce the left- and right-handed circularly polarized light required to produce spin polarized electrons.

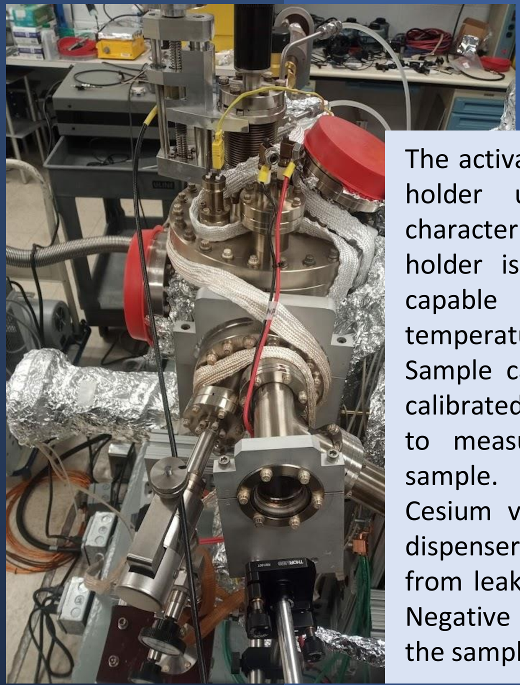

The activation chamber hosts the sample holder used during activation and characterization of the samples. The holder is equipped with a BN heater capable of bringing the samples to temperatures above 600 C.
Sample can be negatively biased and a calibrated K Type thermocouple is used to measure the temperature of the sample.
Cesium vapors from a metal chromate dispenser and high purity oxygen coming from leak valve are used to perform the Negative Electron Affinity activation of the samples.

SMI Led Team's innovative solution

GaAs	5 nm	$p = 5x10^{19}\ cm^{-3}$	
$GaAs_{0.62}P_{0.38}$	4 nm	$p = 5x10^{17}\ cm^{-3}$	30 pairs
GaAs	4 nm	$p = 5x10^{17}\ cm^{-3}$	
$GaAs_{0.81}P_{0.19}$	300 nm	$p = 5x10^{18}\ cm^{-3}$	
$AlAs_{0.78}P_{0.22}$	65 nm	$p = 5x10^{18}\ cm^{-3}$	10 pairs
$GaAs_{0.81}P_{0.19}$	55 nm	$p = 5x10^{18}\ cm^{-3}$	
$GaAs_{0.81}P_{0.19}$	2000 nm	$p = 5x10^{18}\ cm^{-3}$	
$GaAs\text{->}GaAs_{0.81}P_{0.19}$	2750 nm	$p = 5x10^{18}\ cm^{-3}$	
GaAs buffer	200 nm	$p = 5x10^{18}\ cm^{-3}$	
GaAs substrate		$p > 1x10^{18}\ cm^{-3}$	

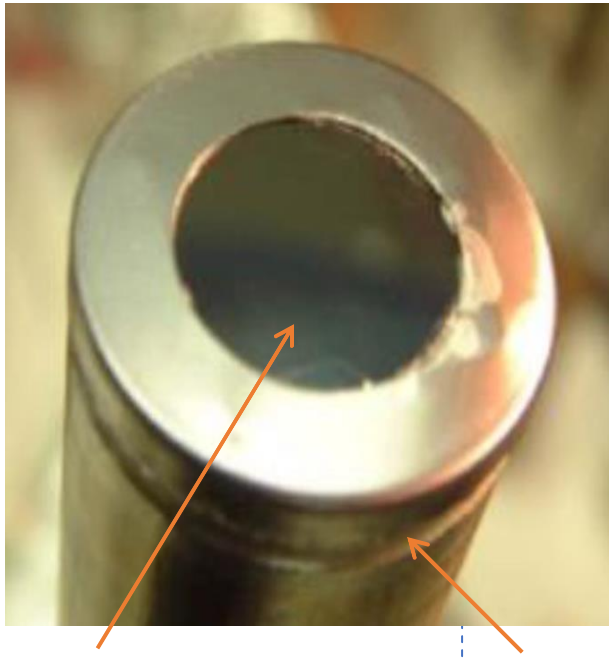

- *Highly efficient spin polarized narrow energy distribution electron source emits electrons upon excitation by a circularly polarized laser beam with energy close to the energy band gap requiring negative electron affinity (NEA) at the surface of the semiconductor:*
- *BNL designed super lattice distributed bragg reflector (SL-DBR) structure uses strain compensation to mitigate relaxation of strained layer*
- *This allows for increased number of SL pair for increased optical absorption and hence increased QE*
- *Due to the reduced strain (+/- 0.7%) Heavy Hole and Light Holes are separated by only ~66 meV*

Major Goals and Objectives of this Project

- Refine device design and model-through material and device characterization/performance feedback – with a focus on tuning composition, superlattice (SL) and DBR/F-P layer thicknesses; as appropriate to maximize QE, ESP and lifetimes for operation at 780 nm.
    - Target Performance Parameters
        - ESP – 90%
        - QE – 5 %
- Mitigate/eliminate oxide formation on top of the device which is suspected/anticipated to decrease the QE and ESP of the photocathode (Starting by using vacuum packaging) and understand impact on ESP if any.
- Refine structure tuning to provide optimal performance at 780 nm.
- Determine the commercializable performance specifications of the photocathodes through testing (QE, upper current limit, ESP, operational lifetime, bunch charge achievable, packaging and preparation and compare to commercial values.
- Demonstrate high performance spin polarized photocathodes at BNL testing laboratory and potentially sample to other interested groups – including Jefferson National Lab, Cornell University, and others yet to be determined or suggested by DOE.
- Refine Phase III production and commercialization pathways – evaluate additional market.

Growth of GaAs/GaAsP SL on base structure

- $GaAs_{0.81}P_{0.19}$ composition, growth rate and doping were calibrated, and base structures were grown.
- Following this $GaAs_{0.62}P_{0.38}$ was calibrated, and SL structures were grown and optimized on existing base structures.
- Wafers, with full structure except DBR, were sent to BNL for testing.

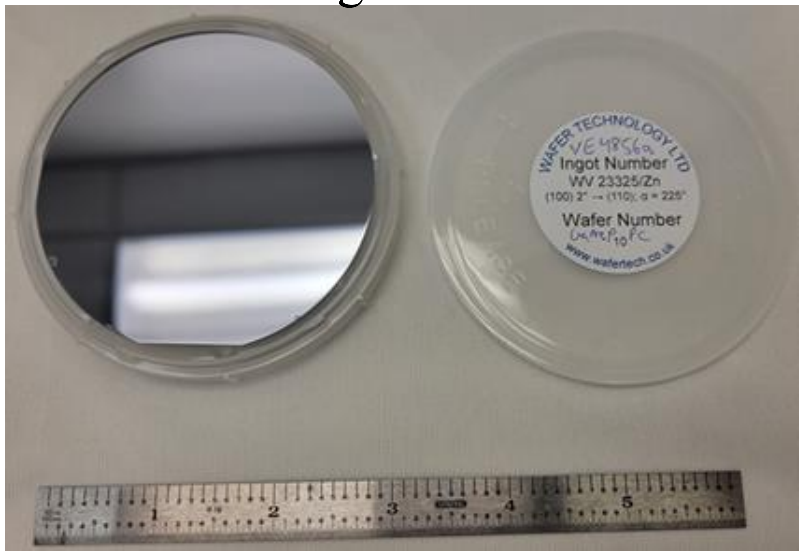

Photograph of 3-inch full wafer structure except DBR

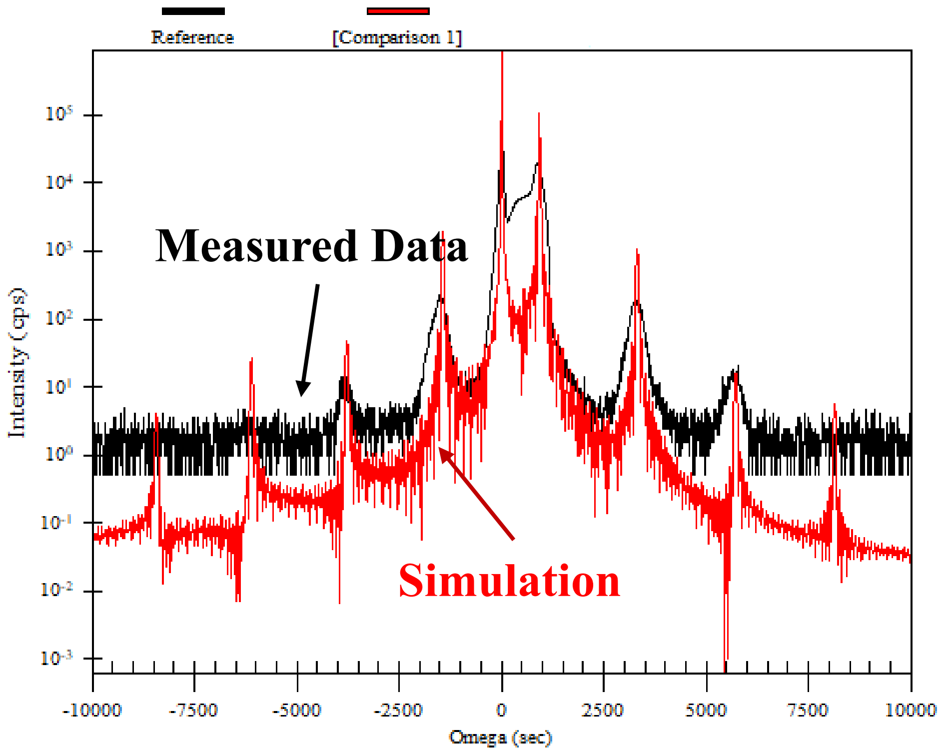

X-ray measured data (black) compared to simulation (red) of full structure except DBR. The measured peak spacing and position match up indicating thickness and composition is close to simulation data.

DBR calibration

- $AlAs_{0.81}P_{0.19}$ was calibrated and wafers of DBR on base structure were grown.
- Thickness was adjusted to target reflectance at 780 nm.

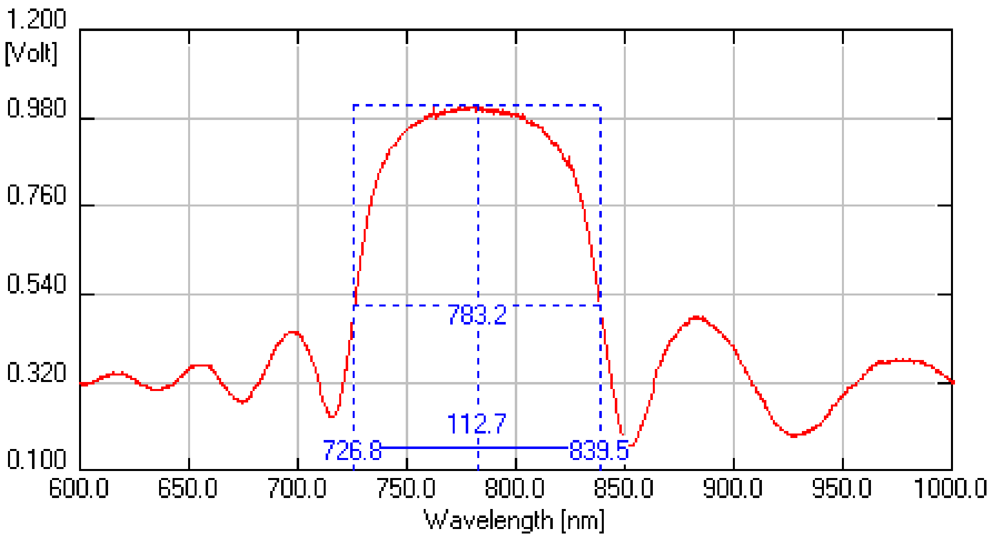

Reflectivity of DBR regrown on base wafer centered near target 780 nm.

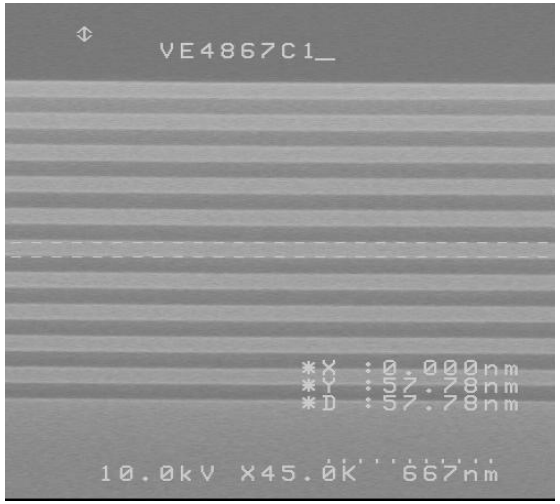

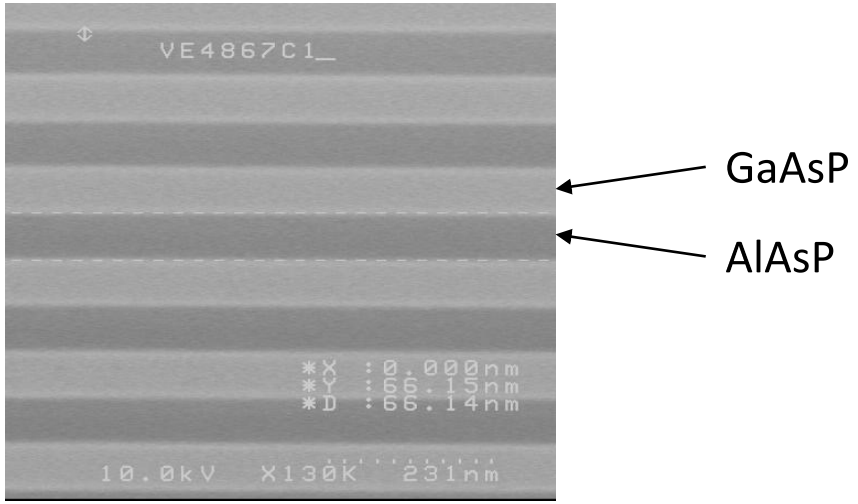

SEM image of cross section of DBR calibration run shows good uniformity and correct layer thicknesses.

ESP & QE Photocathodes Results

ESP and QE Vs Wavelength for sample with DBR

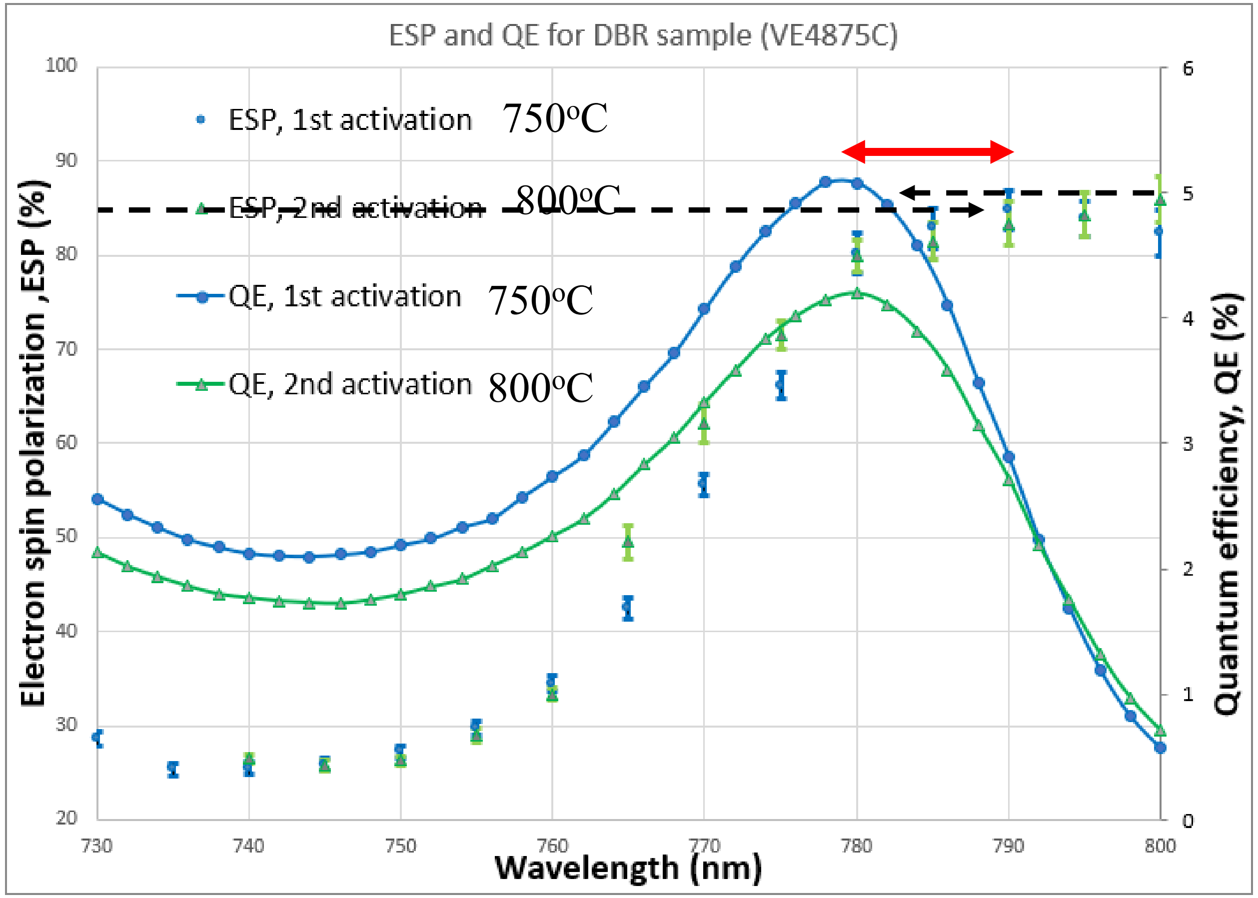

Sample is not Arsenic (As) capped and oxide is likely formed at the DBR-SL interface and surface.

Heat clean at <600 C will likely not remove all oxide (reported temperatures are for the heater not the sample).

QE> 5%

ESP> 85%

To meet SBIR ideal specs:
Align the peaks ~780
Increase QE >5% (if not 10%)
and push ESP >90%

Phase I&II Approach to Increase ESP and QE

Phase I demonstrated base calculated structured with great success. Several parameters have been tested to further improve ESP, QE, and structure reproducibility. The rationale is as follows:

- **C doping** was tested as literature reports indicate larger optical absorption compared to Zn-doped layer;
  - Zn does not incorporate easily in DBR AlAsP layers;
- **Performed 1-step growth:** no interruption (for measurement) between DBR and SL layers to mitigate possible contamination;
- **Tested modified SL-DBR structures** that uses a slightly larger strain (± 0.8%) which increases HH-LH separation up to ~77 meV;
- **Increased the number of DBR layers** to further increase the reflectivity;
- **Sealed packaging of wafers** to mitigate surface oxidation and facilitate NEA formation during activation.
- Phase II focused on refinement to theory, structures overall refinements, and reproducibility.

Best of ESP & QE data

	QE (%)	ESP (%)	FoM=QExESP^2
SMI	4.5	85	3.26 % @ 780 nm
SMI	13.5	65	5.70 % @ 790 nm
SMI	5.5	82	3.70 % @ 790 nm
Others			
BNL/SNL	15.5	62	5.96% @ 776 nm
JLab	2.9	82	1.92% @ 785 nm

Pictures from left full structures sealed in N2 and never exposed to air, Full structures used for characterization and exposed to air and calibration structures.

References:

1. Jyoti Biswas, Luca Cultera, et al., AIP Advances 13, 085106 (2023).

2. W. Liu, et al., Appl. Phys. Lett. 109, 252104 (2016).

3. B. Belfore et al., Appl. Phys. Lett., DOI: 10.1063/5.0170106

Batch 1: Photocathode Structures

- Explored C doping rather than Zn for higher QE: This investigation into using C as a dopant instead of Zn to improve the QE of the device.
- Nitrogen package to mitigate surface oxidation: A "nitrogen package" to prevent the surface of the material from reacting with oxygen (oxidation), which can degrade performance.
- Different design with increased P content (up to 44%) for higher heavy hole (HH)- light hole (LH) separation: This batch utilized a modified design where the P content in a specific layer was significantly increased (up to 44%). The purpose of this increase was to achieve a higher "Heavy Hole-Light Hole (HH-LH) separation”, which can influence device performance characteristics like polarization.

Batch 1 photocathode test data

XRD

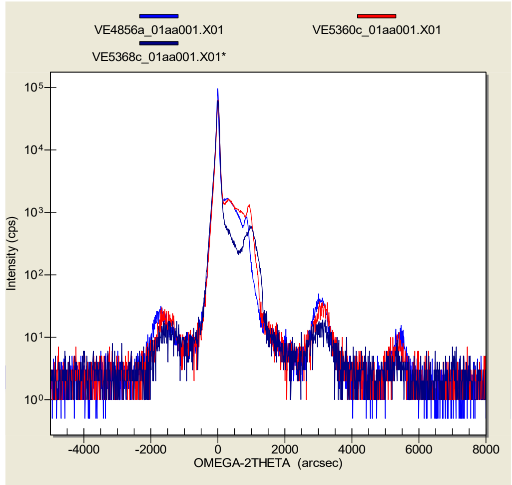

PL

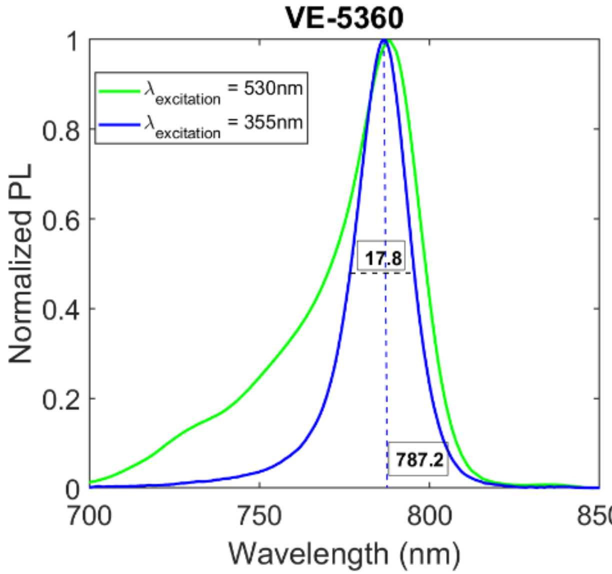

QE spectral response

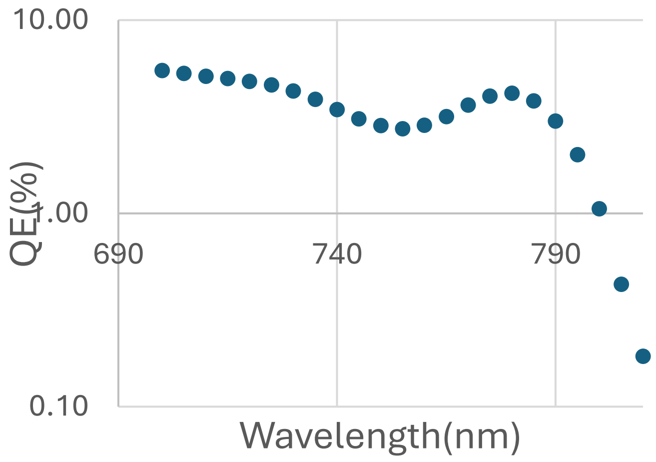

Morphology measurement

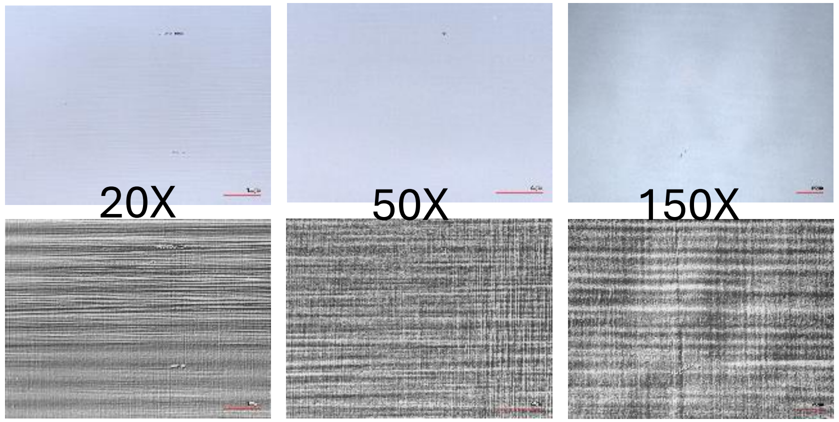

ESP spectral response

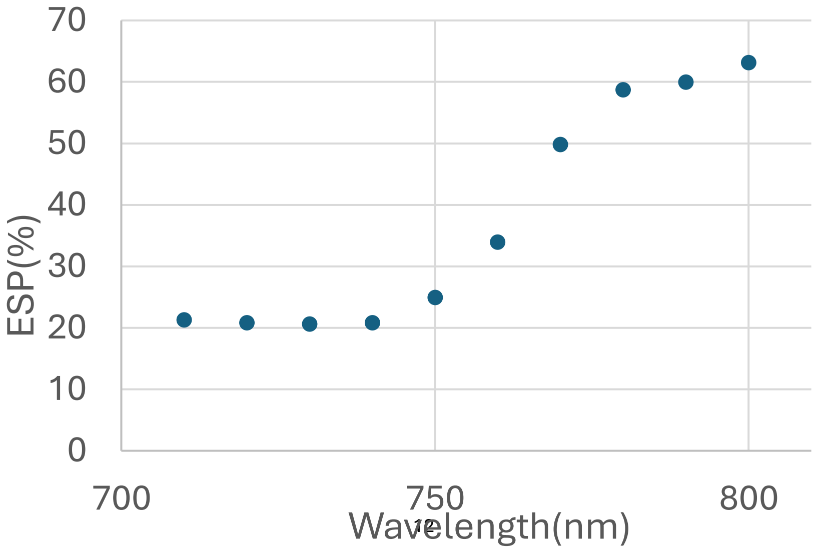

Summary of ESP from cathodes of Batch 1

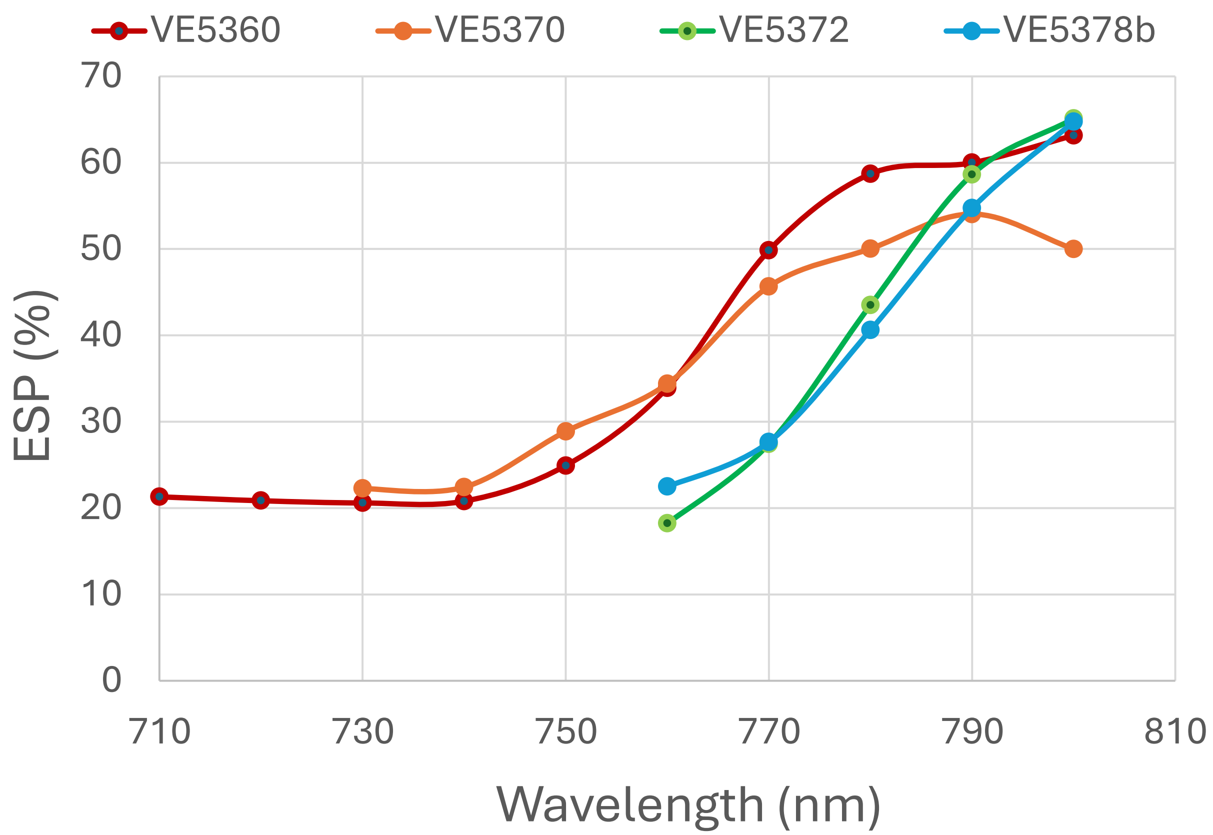

A redesigned structure, featuring increased Phosphorus (P) content (up to 44%) to enhance Heavy Hole-Light Hole (HH-LH) separation, unfortunately led to low ESP. A potential explanation for this reduced ESP is that the elevated P content may have amplified the lattice mismatch, thereby compromising the interface quality of the subsequent layers.

Batch 2: Change of SL structure

- Increase in the P concentration in the pseudo-substrate: **19%** to **22%**
- Increase P concentration in the SL: **38%** to **44%**
- Simulations predict an increase in **HH-LH separation: 66 meV** to **77 meV**

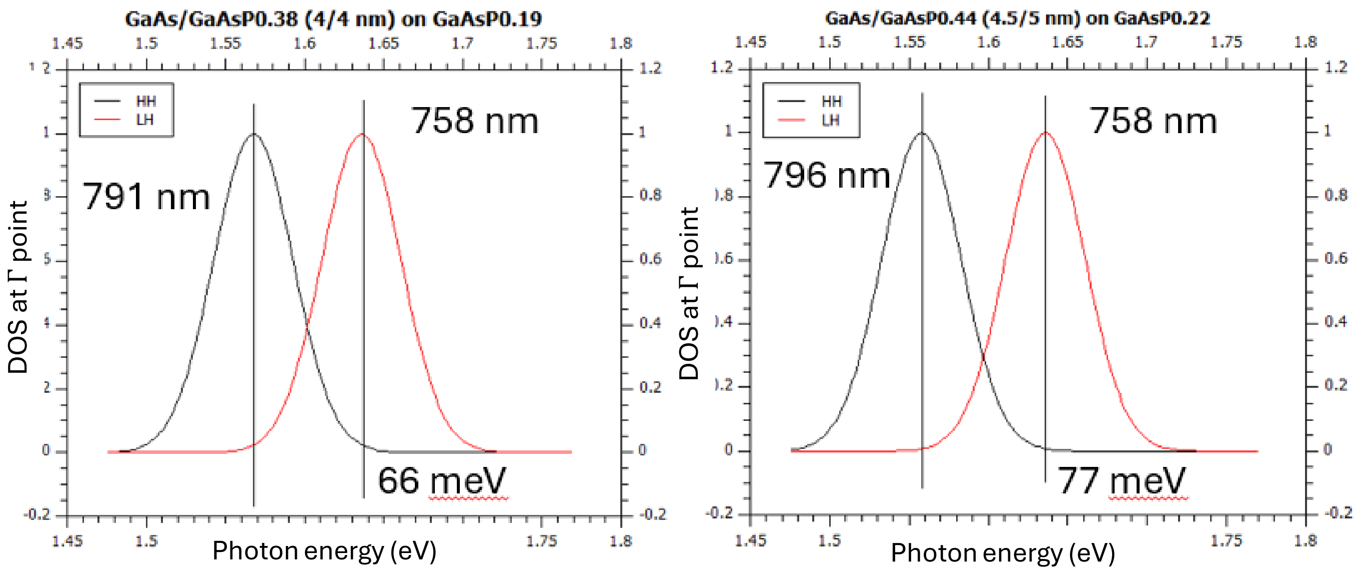

Test results from Batch 2 photocathodes

XRD

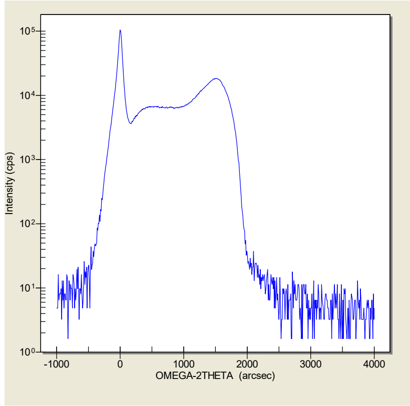

PL spectra

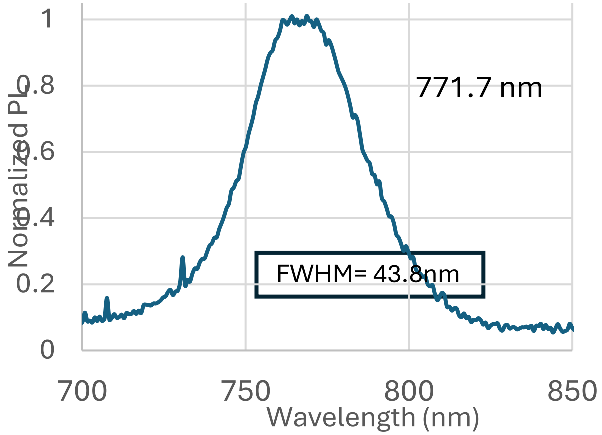

QE spectral response

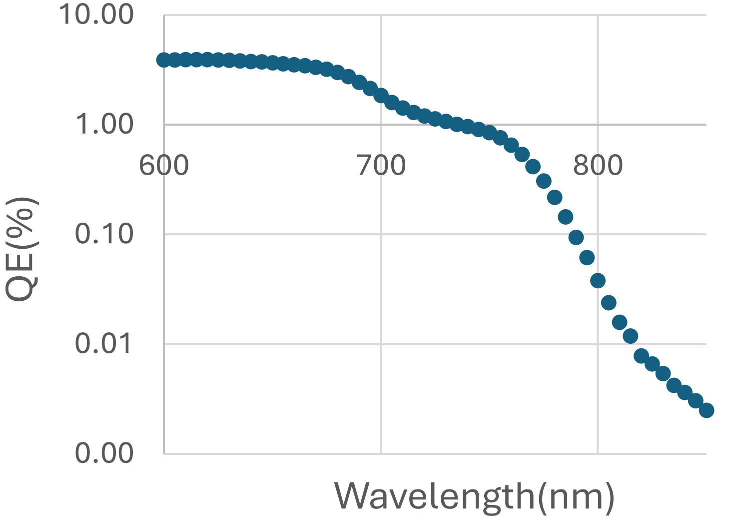

Morphology profile

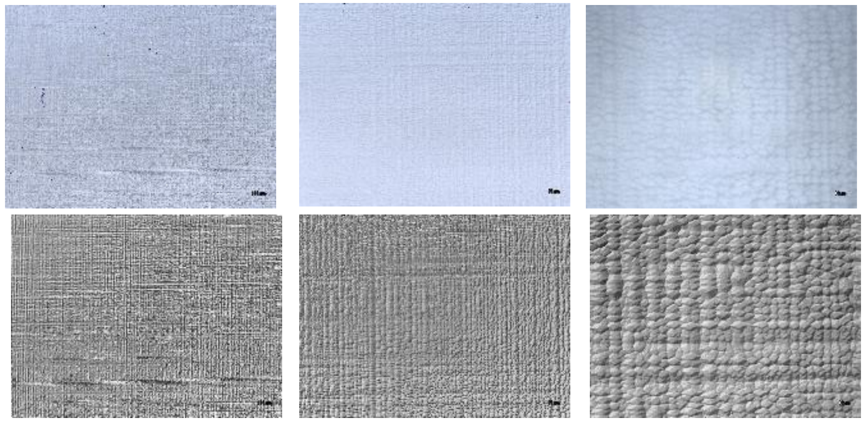

20X 50X 150X

Higher roughness is visible, which probably leads to depolarization

ESP spectral response

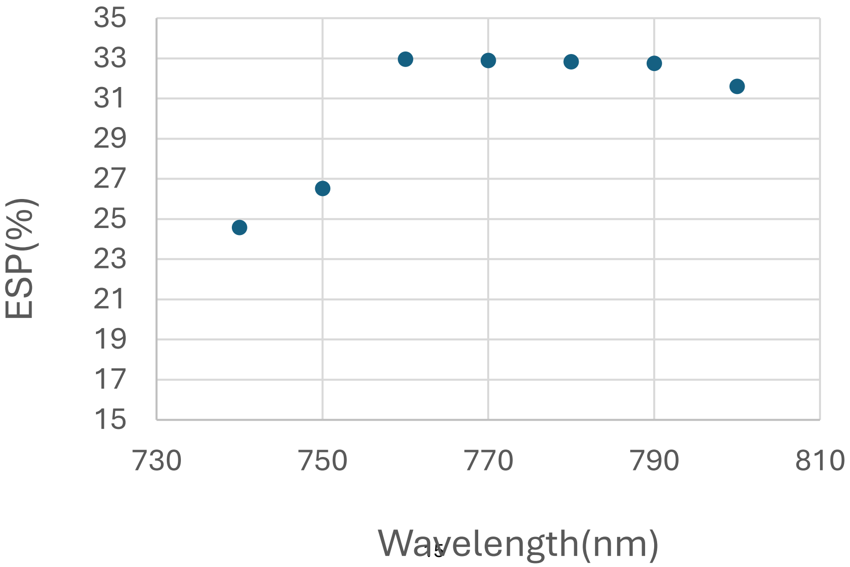

Summary of ESP from cathodes of Batch 2

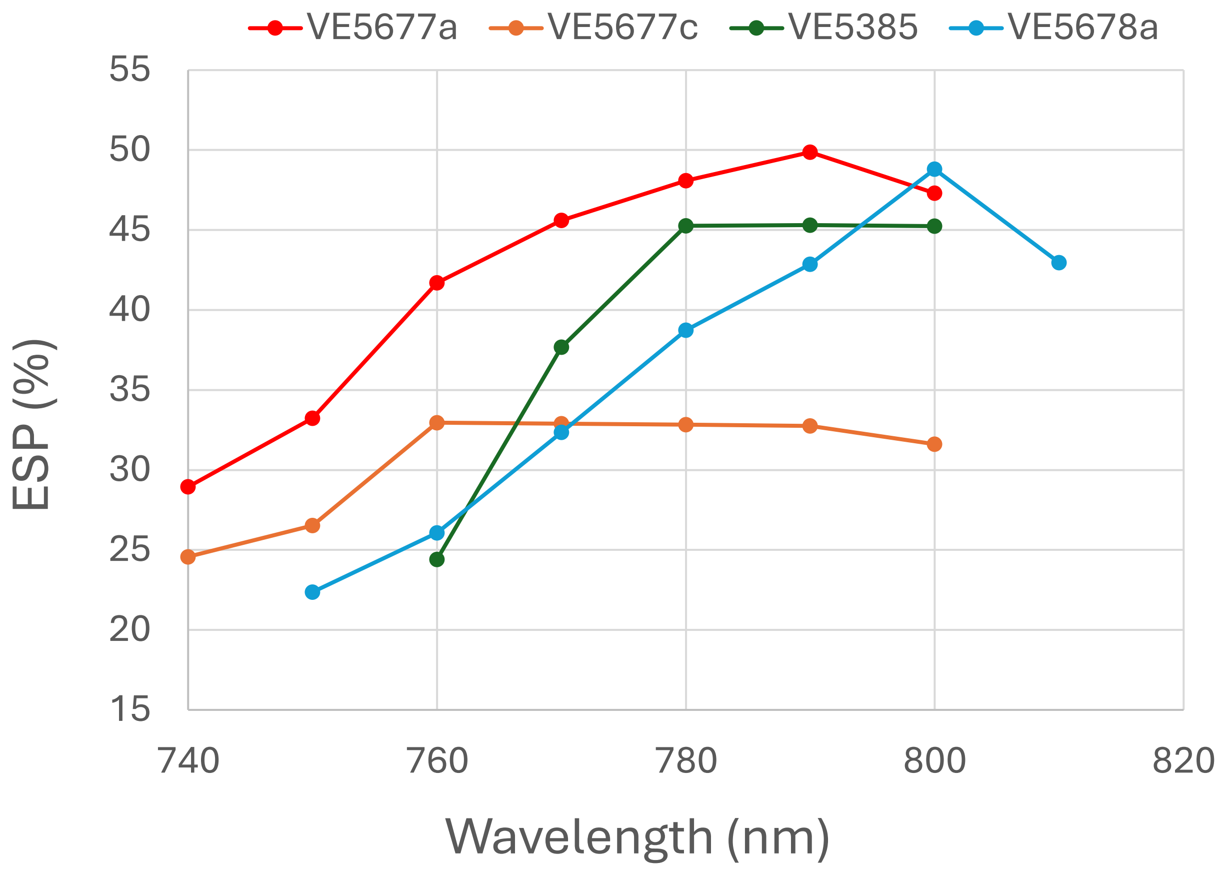

Spacer layer description:

- VE5677a - GaAsP28
- VE5677c - GaAsP28
- VE5385 - GaAsP22
- VE5678a - GaAsP19

Photocathodes with elevated phosphorus (P) content in the buffer layer exhibit higher ESP at shorter wavelengths, as their ESP decreases more gradually compared to cathodes with lower P content. However, GaAsP cathodes with 28% P show lower overall ESP, likely due to increased surface roughness in the pseudosubstrate, as observed in surface morphology maps.

Comparison of ESP performance from samples grown on same wafer using different buffer/spacer

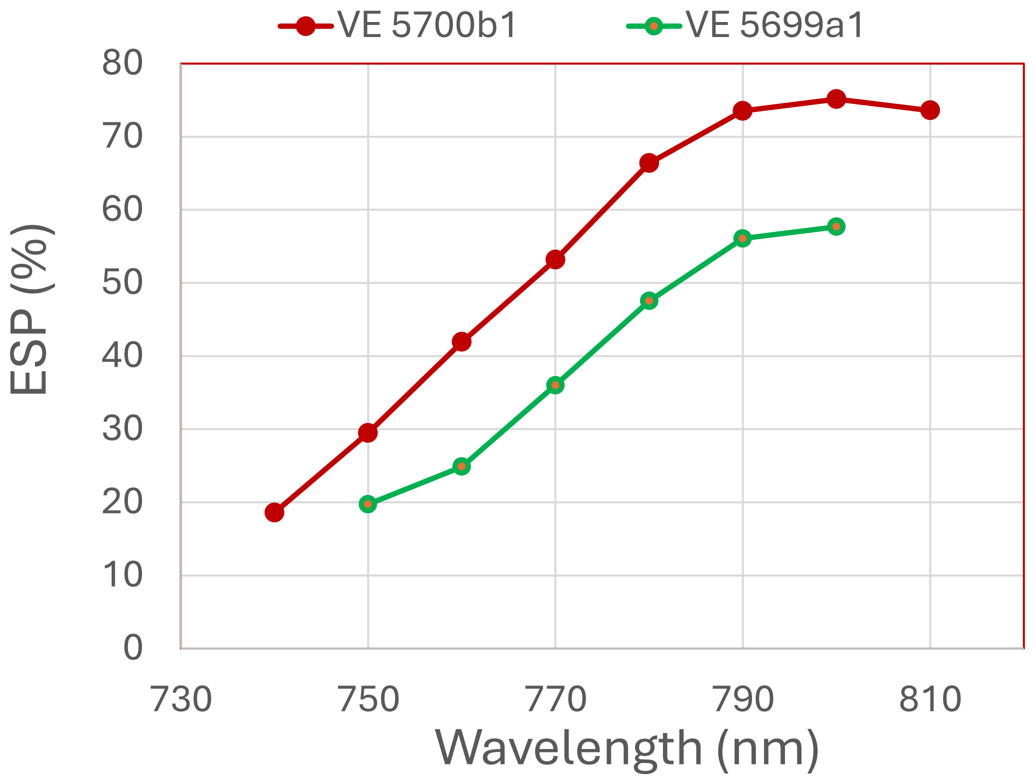

Description of spacer layer:

- VE 5699a1: GaAsP19
- VE 5700b1: Al10GaAsP19

Higher ESP observed from cathode with $Al_{10}GaAsP_{19}$ as spacer, which supports the idea that this **spacer layer acts as a barrier to the diffusion of electrons into the superlattice layers**; thereby preventing any dilution of spin polarization of electrons emitted from the GaAs wells in the SL.

Comparison of ESP performance from the samples with highest ESP from different batches 1, 2 and 3

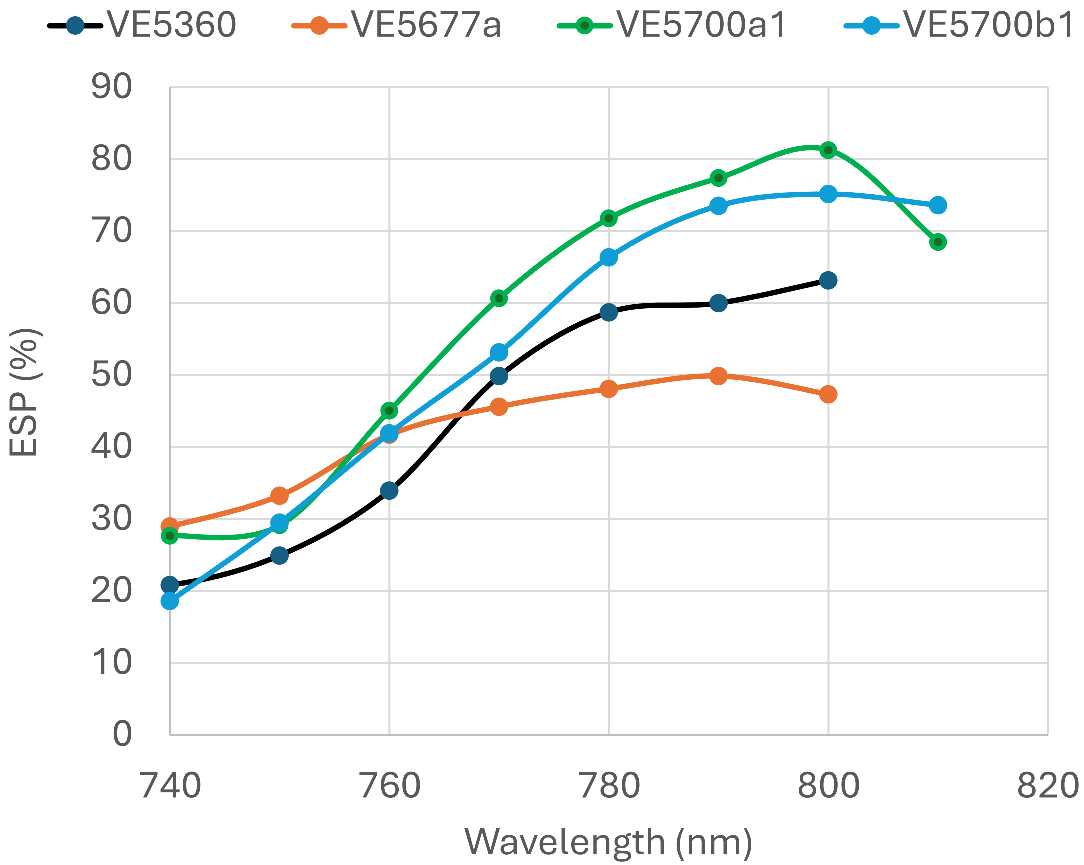

Description of spacer layer:

- VE5360 - GaAsP19
- VE5677a - GaAsP28
- VE5700a1 - Al10GaAsP19
- VE5700b1 - Al10GaAsP19

- Highest ESP observed from cathodes, which uses $Al_{10}GaAsP_{19}$ as the spacer layer.
- Increasing the P conc. in the spacer layer increases the ESP at shorter wavelengths but due to increased surface roughness overall ESP is lower from cathodes with higher P conc.

Batch 4 Photocathode testing

Photoluminescence

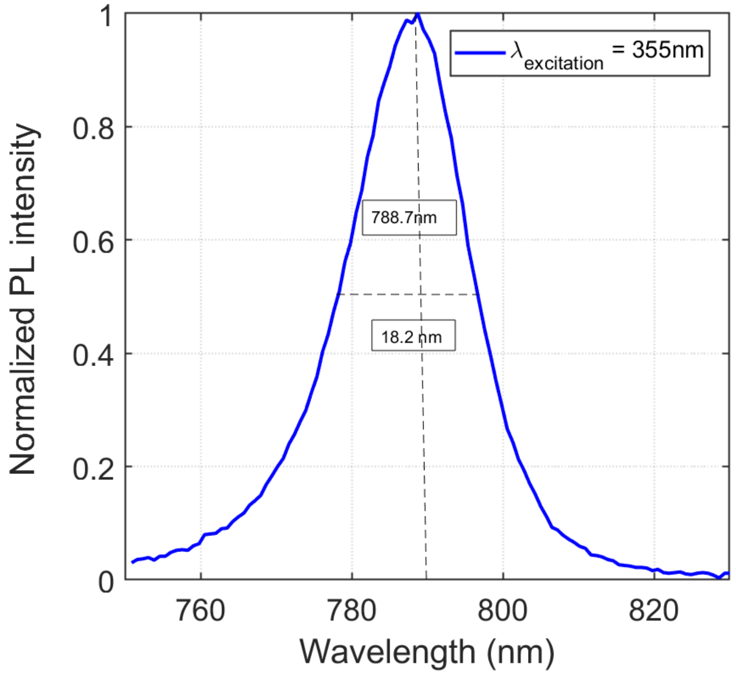

QE spectral response

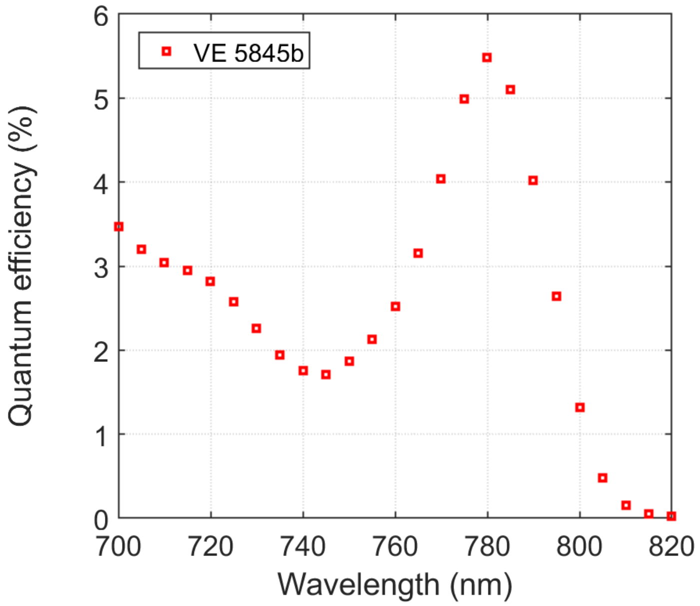

Morphology

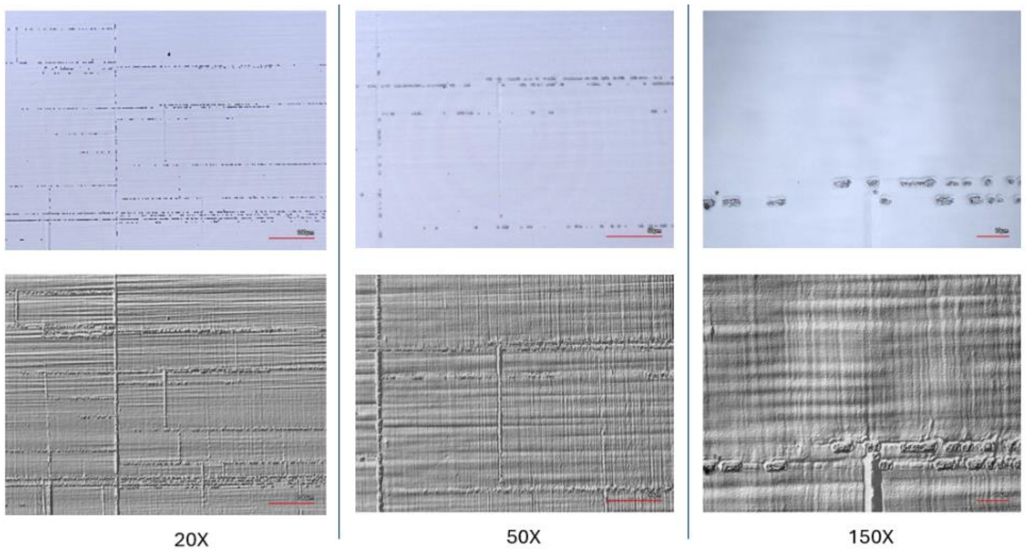

ESP spectral response

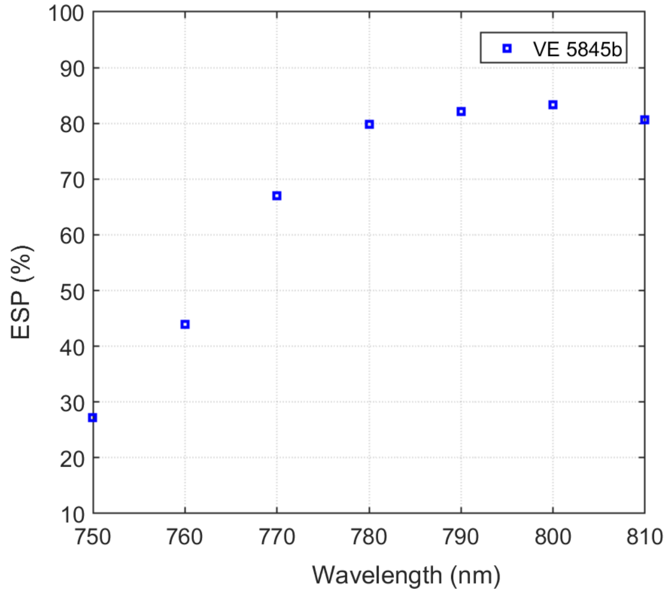

SMI VE5841b: buffer GaAsP19

PL

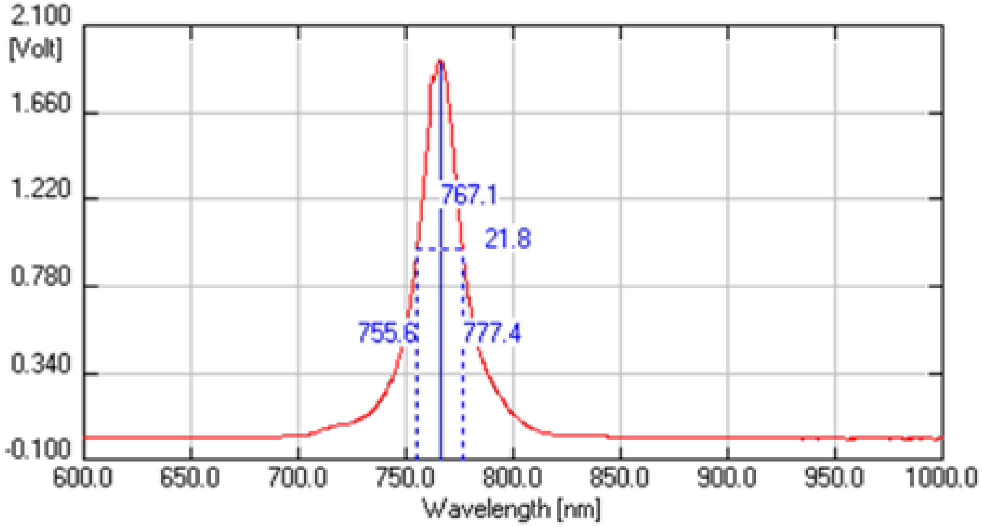

QE spectral response

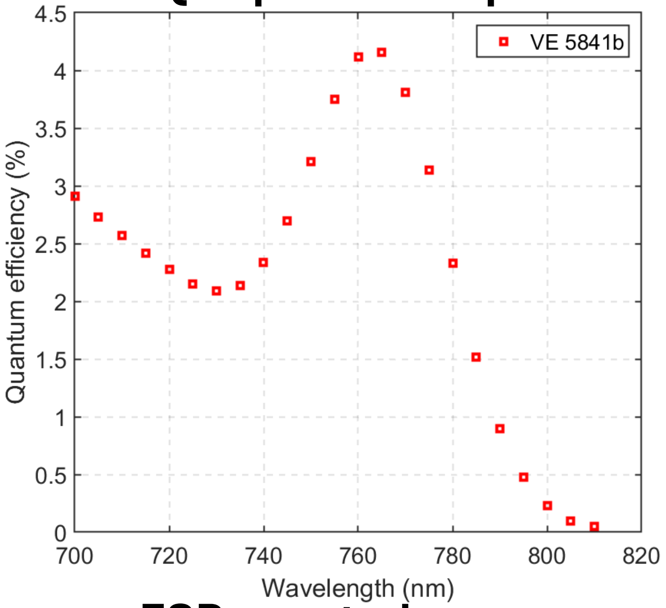

Morphology

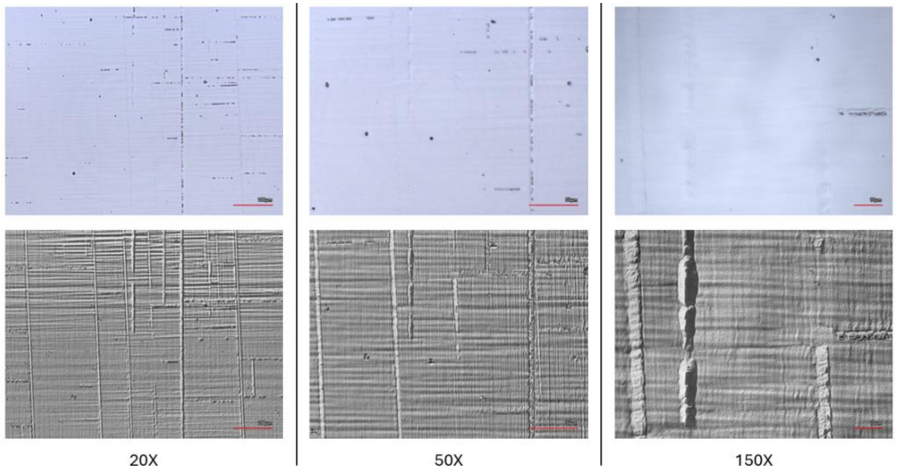

ESP spectral response

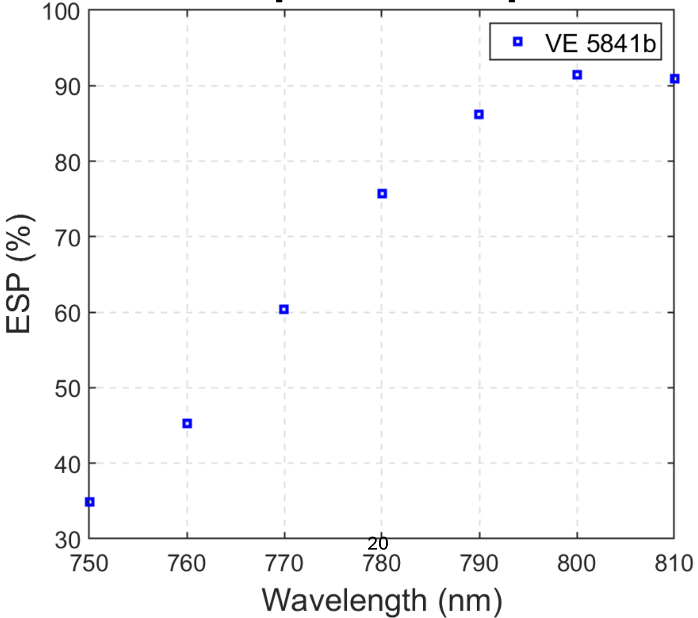

ESP & QE performance comparison – Phase I vs Phase II

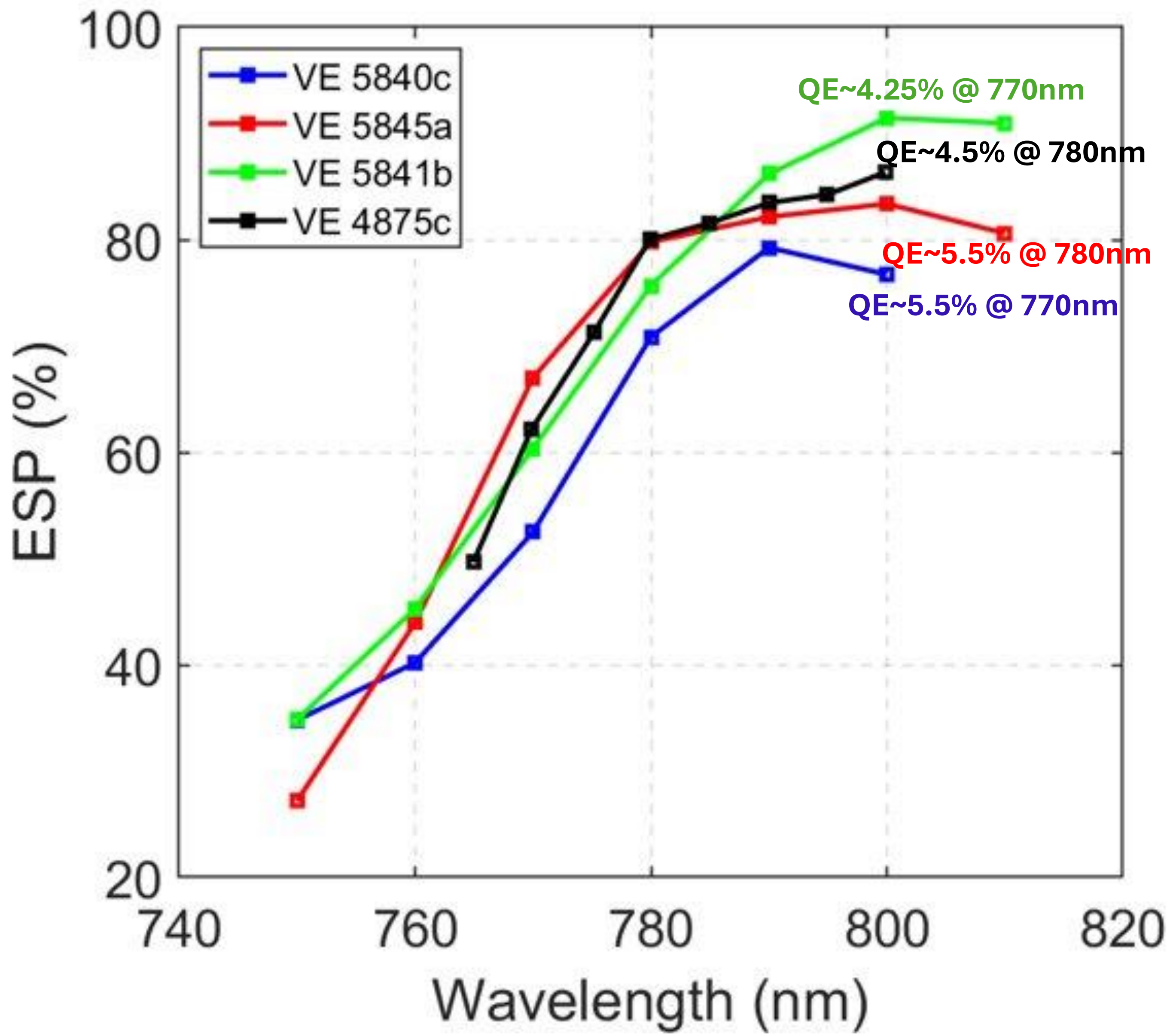

Description of spacer layer:

- VE5841b - GaAsP19
- VE5840c - GaAsP19
- VE5845a - Al15GaAsP19
- VE4875c - GaAsP19 – Phase I

Sample No.#	ESP (%)	QE (%)	Fluence of Spin Polarized Electrons per 100 Incident Photons
VE5841b	92	4.25	3.91
VE4875c	85	4.5	3.825 (Phase I)
VE5845a	82	5.5	4.51
VE5840c	79	5.5	4.345

Phase II: Net ESP/photon is > 15% higher than Phase I

Outline of results and observations

We learned several things that influence the performance of the photocathode:

Phase I: Initial Growth and SL-DBR Structure Testing

We successfully grew and tested the SL-DBR structure, demonstrating an ESP greater than 80% at wavelengths longer than 790 nm and a QE exceeding 4.5% at 780 nm.

Phase II: Advanced Material Development and Optimization

(a) Replacement of C doping in place of Zn – no observable impact.

(b) Nitrogen packing: Improves QE

(c) High P (44% from 19%) to increase HH-LH separation to increase ESP – High QE but net reduced ESP due to surface degradation due to lattice mismatch.

(d) P at 28% - interface quality in the superlattice still compromised resulting in low ESP.

(e) Increase the bandgap of the spacer layer by adding Al to GaAsP layer between the DBR and FP superlattice structures which was expected to prevent spin polarized electrons from reabsorbed in the DBR layers – Did result in increased ESP.

(f) Added AlGaAsP spacer layer to the Phase I structure – got high ESP and QE.

Summary

- Our initial efforts in Phase I established a robust baseline, achieving **85% ESP** and a **4.5% QE**. These results provided a strong foundation for further exploration and optimization.
- **Phase II Exploration: Pushing the Boundaries**
- Building on the successes of Phase I, our objectives for Phase II focused on exploring the device growth and structure phase space to concurrently enhance both ESP and QE.
- **Superlattice Strain Experimentation**
- During Phase II, we investigated the impact of increasing strain within the superlattice structure. This strategic adjustment yielded significant improvements in quantum efficiency, with **QE reaching as high as 13%**. While this demonstrated a promising avenue for QE enhancement, it unfortunately came at the cost of reduced ESP.
- While confined in design analysis we can also infer that minor composition changes and DBR thickness variations can greatly affect performance in the future production tool would benefit the works with greater in-situ feedback
- **Returning to the Phase I Structure: Optimizing for Balance**
- Recognizing the need to maintain high ESP while improving QE, we decided to Phase I incorporation of an Phase II **AlGaAs spacer layer**. This decision proved beneficial, allowing us to successfully demonstrate **ESP > 80%** while simultaneously achieving a QE of ~ **5.5%**. This represents a significant step forward, showcasing our ability to balance critical performance metrics.
- Last few tests are scheduled in the following months are a. Test remaining wafers & b. BNL will measure a sample in its gun in the accelerator facility.

Next steps…

- **Send samples to DOE labs for characterization** of spin-polarized photocathodes.
- Test Photocathodes in actual accelerator gun at BNL (planned pending system availability) and other facilities.
- To significantly advance the performance of spin-polarized photocathodes, **Phase IIB** if possible, with funding from the DOE.
- To fully validate our findings and ensure the robustness of our structure – **Optimize uniformity and Set quality control for commercialization**.
- This will represent a substantial step towards meeting the high-performance requirements for future spin-polarized electron sources in various DOE and other applications.

THANK YOU

Structured Materials Industries, Inc.
www.smicvd.com

PI: Dr. Kannan Vasudevan
Scientist
&
Dr. Gary S Tompa
President
Phone: 732 302 9274
Email: v.kannan@structuredmaterials.com; sales@structuredmaterials.com

SMI Provides Complete Solutions

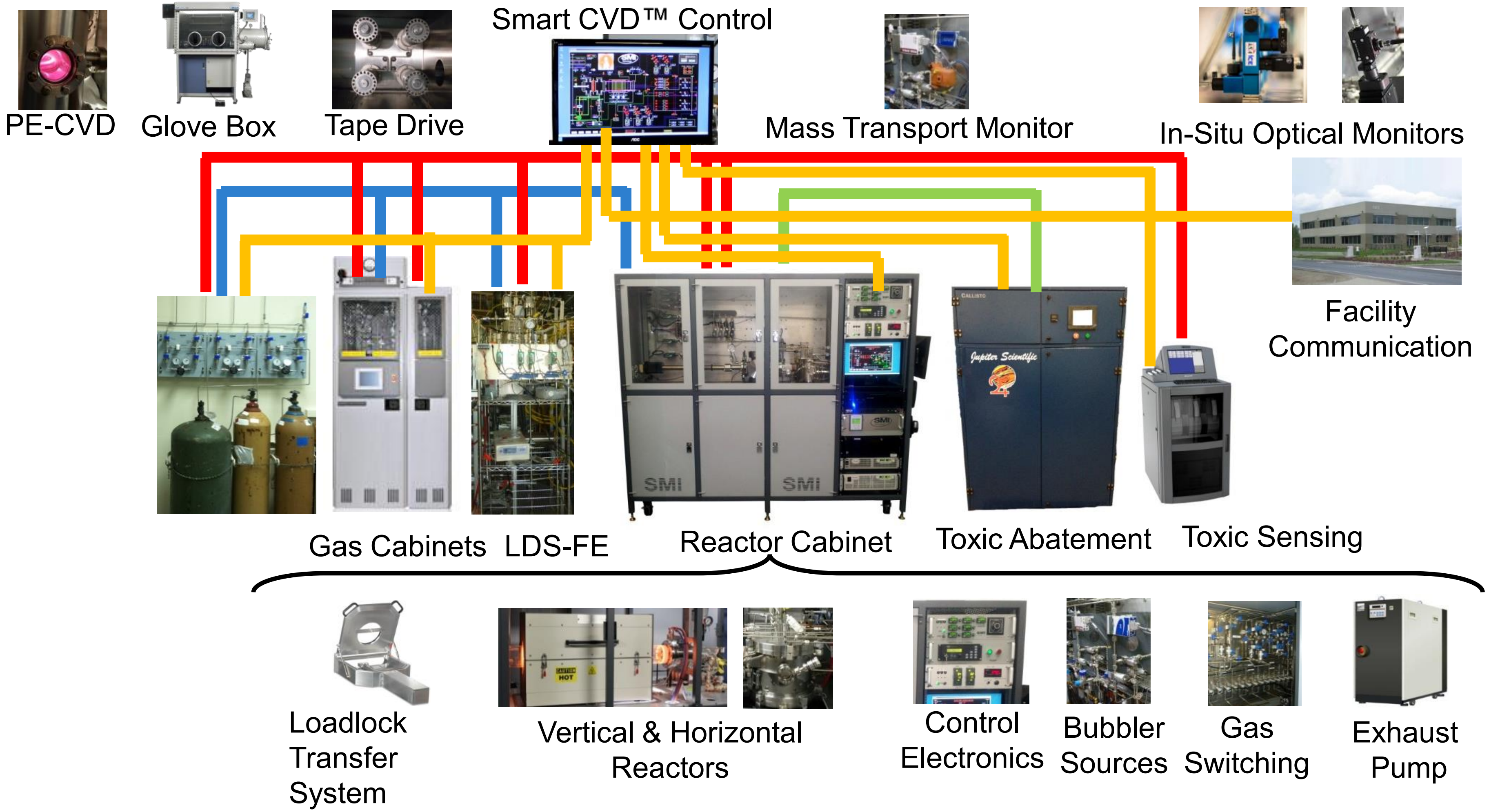

>70 Tools Fielded: SMI Enables Technology

Vertical

2400C

Oxides

High Pressure

Anneal

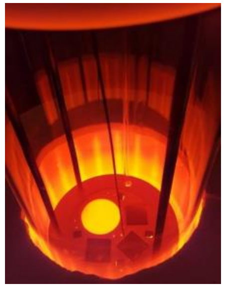

VLSI

Horizontal 2D

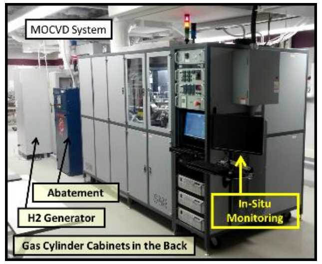

III-V- II/VI

ALD

Cluster Tool

FB - CVD

HTS Tape

Nitrides / Carbides

Rebuilds & Conversions

ICP-CVD

Diamond -- Annealing -- Components -- Design Services -- Contract Research: Commercial & Government

Control Systems: Process Control Features
Digital and Analog System

Well Controlled Process – Reproducible Product

Standard Features:

- Low Cost
- Based on commercial software products
- Graphical User Interface in Microsoft Windows environment
- Real time interactive mimic panels of the process system
- Spread sheet interface for process configuration
- Advanced alarm monitoring and management
- Password protection for operator interface

Optional Features

- Real time data logging and displaying
- Network support for distributed control system
- Automated process documentation generation
- Flexible hardware interface (PLCs, commercial instruments, etc...)
- In-Situ Process Monitoring and Interactive Control
- On-Line (Remote) operation, diagnostics, and upgrades
- Maintenance Procedures- Resource Consumption
- Sample/Wafer Tracking
- MECS/SECS Compatibility
- Remote access beyond networking

SMI Fabricated Devices & Structures

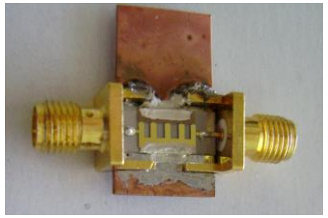
Tunable X-Band Filter

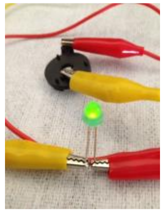
Battery made from Cathode Material

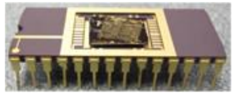
InN/Graphene Gas Sensor


Display Electrodes


SuperConductor Tapes

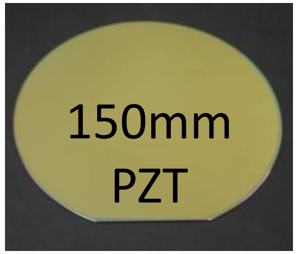


Graphene Sensor

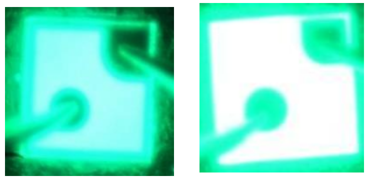
Superior LED Contacts


Missile ARCs

SRAMs and FRAMs


Light Culminating Reflectors

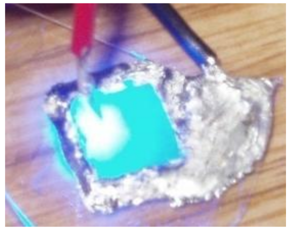
Blue LED with ZnO Contacts

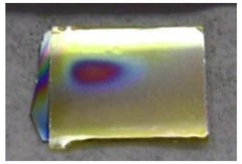
CBRAM GeS: Ag on polymer ceramics


Bulk Crystal Fabrication

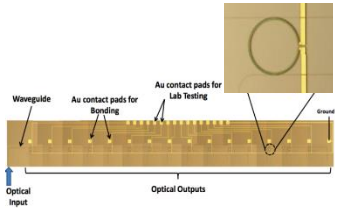

Si Photonics


GE Dome Coating


FB-CVD coated with $Ti_{0.5}Si_{0.5}O_2$

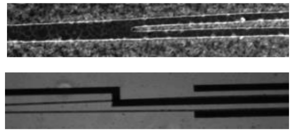
LiNbO3 Waveguide Modulator

CNT Structures SMI Logo in CNTs

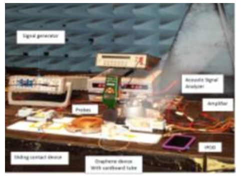
Graphene Speaker

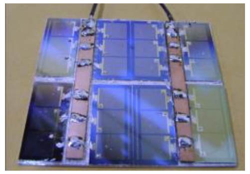
PhotoVoltaics & ThermoPhotoVoltaics

SMI International Commitment to Customer Excellence